

Born-model predictions for $\gamma\gamma \rightarrow \rho^\pm \pi^\mp$

E. Bagan, A. Bramon, and F. Cornet

Departament de Física Teòrica, Universitat Autònoma de Barcelona, Bellaterra, Barcelona, Spain

(Received 23 October 1981; revised manuscript received 18 December 1981)

The main features of $\gamma\gamma \rightarrow \rho^\pm \pi^\mp$ are studied in terms of a gauge-invariant (Born) amplitude constructed from the phenomenological $\rho^\pm \rightarrow \pi^\pm \gamma$ coupling. Large cross sections are predicted and the possibility of determining the ρ^\pm -meson magnetic moment is considered.

I. INTRODUCTION

Much effort has recently been devoted to the experimental study of photon-photon annihilations into hadrons at PETRA¹ and SPEAR.² As a result, the resonant channels $\gamma\gamma \rightarrow f \rightarrow \pi^+ \pi^-$, $\gamma\gamma \rightarrow f \rightarrow \pi^0 \pi^0$, $\gamma\gamma \rightarrow A_2 \rightarrow \eta \pi$, $\gamma\gamma \rightarrow \eta' \rightarrow \pi^+ \pi^- \gamma$, and $\gamma\gamma \rightarrow S^* \rightarrow \pi^+ \pi^-$ have been unambiguously observed and the couplings of these $J^{PC} = 2^{++}, 0^{-+}$, and 0^{++} resonances to $\gamma\gamma$ have been measured.^{1,2} Similarly the nonresonant background to the $\gamma\gamma \rightarrow \pi\pi$ transitions^{1,2} and a large threshold enhancement³ in $\gamma\gamma \rightarrow \rho^0 \rho^0 \rightarrow \pi^+ \pi^- \pi^+ \pi^-$ have been observed. Data on other hadronic channels, such as $\gamma\gamma \rightarrow \pi^+ \pi^- \pi^0$ (possibly dominated by $\gamma\gamma \rightarrow \rho\pi$), are expected to become available in the near future.

From the theoretical point of view, a simple (gauge-invariant) Born model⁴ accounts for the background observed in $\gamma\gamma \rightarrow \pi^+ \pi^-$ (Ref. 2) and obvious generalizations of the model have been proposed to explain [in terms of the channels $\gamma\gamma \rightarrow \rho\pi^+ \pi^-$ (Ref. 5) and $\gamma\gamma \rightarrow f\pi^+ \pi^-$ (Ref. 6)] the large values of the recently measured cross section³ for $\gamma\gamma \rightarrow \pi^+ \pi^- \pi^+ \pi^-$. In the resonance or low-energy region, this Born-term background will be modulated by the different resonant peaks and, possibly but much more speculatively, by low-mass gluonic states (glueballs) coupled to $\gamma\gamma$ if they exist. At higher energies or momentum transfers, two-photon annihilation into hadrons is expected to provide other valuable tests of quantum chromodynamics⁷ concerning, for instance, the pointlike coupling of photons to the hadronic constituents or the photon structure function.

The purpose of this paper is to study the $\gamma\gamma \rightarrow \rho^\pm \pi^\mp$ transition in the framework of a gauge-

invariant Born model and in the low-energy region, i.e., for total $\gamma\gamma$ center-of-mass energies $W_{\gamma\gamma}$ ranging from $M + m \simeq 0.9$ GeV (M and m are the ρ and π masses, respectively) up to $W_{\gamma\gamma} \simeq 1.6$ GeV. In this range of energy the only known resonance which couples both to $\gamma\gamma$ and $\rho\pi$ is the A_2 meson.⁸ On the other hand, no glueballs are coupled to our negative- G -parity final state. Therefore, the region with $W_{\gamma\gamma} < m_{A_2} \simeq 1.31$ GeV seems an ideal place to study some features of our gauge-invariant set of Born terms and, in particular, the dependence of one of them on the anomalous magnetic moment κ of the charged ρ meson. In this sense, valuable information on κ could be deduced from the measurement of the $\gamma\gamma \rightarrow \rho\pi$ cross section. For energies $W_{\gamma\gamma} \simeq m_{A_2}$ and higher, the contributions from the A_2 and other resonances (such as possible radial excitations of the pion⁹) are expected to appear and modify our results. This could be useful when investigating the existence and properties of such $\rho\pi$ resonant states.

II. GAUGE-INVARIANT AMPLITUDE

FOR $\gamma\gamma \rightarrow \rho\pi$

The Lagrangian densities describing the interactions of photons with charged spin-0 (ϕ, ϕ^\dagger) and spin-1 ($\psi_\mu, \psi_\mu^\dagger$) bosons can be deduced from the corresponding free Lagrangians

$$\mathcal{L}_{\text{free}}^0 = (\partial^\mu \phi)^\dagger (\partial_\mu \phi) - m^2 \phi^\dagger \phi, \tag{1}$$

$$\mathcal{L}_{\text{free}}^1 = -\frac{1}{2} G_{\mu\nu}^\dagger G^{\mu\nu} + M^2 \psi_\mu^\dagger \psi^\mu \tag{2}$$

($G_{\mu\nu} \equiv \partial_\nu \psi_\mu - \partial_\mu \psi_\nu$), by simply introducing the covariant derivatives, $\partial_\mu \rightarrow D_\mu = \partial_\mu + ieA_\mu$, where e ($e > 0$) is the charge of the particle destroyed by ϕ or ψ_μ . One obtains

$$\mathcal{L}_{\text{int}}^0 = -ie [(\partial^\mu \phi) \phi^\dagger - (\partial^\mu \phi^\dagger) \phi] A_\mu + e^2 A^\mu \phi^\dagger \phi, \tag{3}$$

$$\mathcal{L}_{\text{int}}^1 = ie [(\partial^\mu \psi_\nu^\dagger)(A^\nu \psi_\mu - A_\mu \psi^\nu) - (\partial^\mu \psi_\nu)(A^\nu \psi_\mu^\dagger - A_\mu \psi^{\nu\dagger})] - e^2 [A_\mu A^\mu \psi_\nu^\dagger \psi^\nu - A_\nu \psi^\nu A^\mu \psi_\mu^\dagger]. \tag{4}$$

Equation (4) represents the interaction of photons with charged spin-1 bosons having no anomalous magnetic moment κ , i.e., with¹⁰ $\mu = 1 + \kappa = 1$ in units $e/2M$. An anomalous piece can be introduced by adding to Eq. (4) a phenomenological term proportional to the anomaly κ ,

$$\mathcal{L}'_{\text{int}} = ei\kappa F^{\mu\nu} \psi_\mu \psi_\nu^\dagger, \quad (5)$$

which clearly preserves gauge invariance ($F^{\mu\nu} \equiv \partial^\nu A^\mu - \partial^\mu A^\nu$). Then, one obtains the following set of Feynman rules¹⁰:

$$-ie(q_1 + q_2)_\mu, \quad (6a)$$

$$2ie^2 g_{\mu\nu}, \quad (6b)$$

$$ie \{ (p_1 + p_2)_\mu g_{\alpha\beta} - [p_1 + \kappa(p_1 - p_2)]_\beta g_{\mu\alpha} - [p_2 + \kappa(p_2 - p_1)]_\alpha g_{\mu\beta} \}, \quad (6c)$$

$$-ie^2 (2g_{\mu\nu} g_{\alpha\beta} - g_{\mu\alpha} g_{\nu\beta} - g_{\mu\beta} g_{\nu\alpha}) \quad (6d)$$

corresponding, respectively, to the four vertices of Figs. 1(a)–1(d) (to which we refer for notation).

Quite independently, the phenomenological Lagrangian responsible for the well-known radiative transitions $\rho^\pm \rightarrow \pi^\pm \gamma$ (or, similarly, $\omega \rightarrow \pi \gamma$, $K^* \rightarrow K \gamma$, ...) is given by the expression

$$\mathcal{L} = -g \epsilon_{\alpha\beta\gamma\delta} (\partial^\alpha A^\beta) [(\partial^\gamma \psi^\delta) \phi^\dagger + (\partial^\gamma \psi^\delta)^\dagger \phi]. \quad (7)$$

When dealing with charged mesons, the introduction of the covariant derivative generates a new interaction involving an additional (gauge) photon given by

$$\mathcal{L}_{\text{int}} = -ieg \epsilon_{\alpha\beta\gamma\delta} (\partial^\alpha A^\beta) (A^\gamma \psi^\delta \phi^\dagger - A^\gamma \psi^\dagger \delta \phi). \quad (8)$$

From the Lagrangian densities (7) and (8) one easily deduces the Feynman rules for the vertices of Figs. 1(e) and 1(f). They turn out to be, respectively,

$$ig \epsilon_{\sigma\lambda\alpha\mu} k^\sigma p^\lambda, \quad (9e)$$

$$-ige (\epsilon_{\sigma\mu\nu\alpha} k_1^\sigma + \epsilon_{\sigma\nu\mu\alpha} k_2^\sigma), \quad (9f)$$

where the coupling constant g^2 is related to the de-

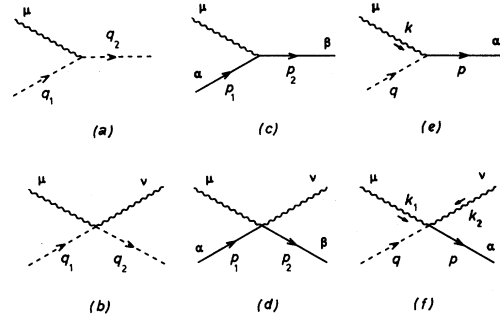


FIG. 1. Graphs corresponding to the Feynman rules [Eqs. (6a)–(6d) and (9e) and (9f)]. Wavy, dashed, and solid lines correspond to photons, spin-0 mesons, and spin-1 mesons, respectively.

coupling width for $\rho \rightarrow \pi \gamma$ through

$$\Gamma(\rho \rightarrow \pi \gamma) = g^2 (M^2 - m^2)^3 / 96 \pi M^3. \quad (10)$$

An independent estimate of g^2 can be obtained from the coupling constant $g_{\rho\omega\pi^2}$ appearing in the $\omega \rightarrow \rho \pi \rightarrow 3\pi$ decay and the vector-meson-dominance (VMD) relation $g^2 = g_{\rho\omega\pi}^2 e^2 / f_\omega^2$. In this context, the different role played by the two photon fields in Eq. (8) (an isoscalar, ω -like photon and an isovector, gauge one) is more transparent. Moreover, the mesonic $\omega\rho\pi$ vertex has the same features (a large coupling constant and the appearance of derivatives of charged fields) as the $\Delta N \pi$ vertex (involving spin- $\frac{1}{2}$ and spin- $\frac{3}{2}$ baryons) which generates an important contact interaction analogous to Eq. (8), dominating the $\gamma\gamma \rightarrow \Delta^{++} \pi^-$ cross section near threshold.⁴ Therefore, it seems reasonable to expect a similar effect in our process $\gamma\gamma \rightarrow \gamma\omega \rightarrow \rho^\pm \pi^\mp$.

It is now a trivial task to obtain the gauge-invariant amplitude for the $\gamma\gamma - \rho^+ \pi^-$ transition corresponding to the three Born diagrams (plus two crossed ones) of Fig. 2. One finds

$$T = eg \epsilon_{\alpha\beta\gamma\delta} [M^{\alpha\beta\gamma\delta}(k, k', \epsilon, \epsilon') + M^{\alpha\beta\gamma\delta}(k', k, \epsilon', \epsilon)], \quad (11)$$

with

$$M^{\alpha\beta\gamma\delta}(k, k', \epsilon, \epsilon') = \frac{\epsilon \cdot (k - 2q)}{2q \cdot k} \epsilon'^\alpha \rho^\beta k'^\gamma p^\delta + \frac{\epsilon \cdot (k - 2p)}{2p \cdot k} \epsilon'^\alpha \rho^\beta k'^\gamma q^\delta + \frac{\mu}{2p \cdot k} [(\epsilon \cdot \rho) \epsilon'^\alpha \epsilon'^\beta \rho^\gamma k'^\delta - (\rho \cdot k) \epsilon'^\alpha \epsilon'^\beta k'^\gamma \rho^\delta] + \epsilon'^\alpha \rho^\beta k'^\gamma \epsilon'^\delta, \quad (12)$$

where k , k' , and p (ϵ , ϵ' , and ρ) are the four-momenta (polarization) of the two photons and the ρ^+ meson, and q that of the π^- .

III. CROSS SECTIONS AND ANGULAR DISTRIBUTIONS FOR $\gamma\gamma \rightarrow \rho\pi$

The differential cross section for unpolarized photons corresponding to the process $\gamma\gamma \rightarrow \rho^+\pi^-$ is given by

$$\frac{d\sigma}{d\Omega} = \frac{1}{32\pi^2} \frac{1}{4} \sum |T|^2 \frac{|\vec{P}|}{W_{\gamma\gamma}^3}, \quad (13)$$

where $|\vec{P}|$ is the momentum of the final particles and the sum extends to all spin states. A straightforward but tedious calculation shows that Eqs. (11) and (12) lead to

$$\sum |T|^2 = e^2 g^2 [A(k, k') + A(k', k)] \quad (14)$$

with

$$A(k, k') = A_0(k, k') + \mu A_1(k, k') + \mu^2 A_2(k, k')$$

and

$$A_0(k, k') = \left\{ \frac{-N}{(q \cdot k)(q \cdot k')} + \frac{2(p \cdot k')^2}{(q \cdot k)^2} [q \cdot (k - q)] \right. \\ \left. + 2 \frac{(k \cdot k')[p \cdot (2q - k')] + 2(q \cdot k')[p \cdot (k' - k)]}{q \cdot k} \right\} + \{p \leftrightarrow q\} \\ - \frac{N}{(p \cdot k)^2} + 2(k \cdot k' - 2p \cdot q) \frac{(p \cdot k')(q \cdot k')}{(p \cdot k)(q \cdot k)} + 2 \frac{(p \cdot k')[p \cdot (k' - k)]}{M^2} - 4k \cdot k', \\ A_1(k, k') = \left[\frac{1}{(p \cdot k)^2} + \frac{1}{(q \cdot k)(p \cdot k)} - \frac{2}{M^2 p \cdot k} \right] N + \frac{2(p \cdot k')[q \cdot (k' - k)]}{M^2} + 2(k \cdot k') \left[\frac{p \cdot q}{M^2} - \frac{q \cdot k'}{p \cdot k} \right], \\ A_2(k, k') = \left[\frac{1}{4(p \cdot k)^2} - \frac{1}{4(p \cdot k)(p \cdot k')} + \frac{1}{M^2 p \cdot k} \right] N \\ + \frac{(q \cdot k')[q \cdot (k' - k)]}{2M^2} + \frac{(k \cdot k')}{2} \left[\frac{m^2}{M^2} - \frac{(q \cdot k)(q \cdot k')}{(p \cdot k)(p \cdot k')} \right],$$

where

$$N = 2(k \cdot k')(q \cdot k)(q \cdot k') - q^2(k \cdot k')^2 = 2(k \cdot k')(p \cdot k)(p \cdot k') - p^2(k \cdot k')^2.$$

The absolute value of the phenomenological coupling constant g can be deduced directly from Eq. (10) and the experimental values¹¹ $\Gamma(\rho^- \rightarrow \pi^- \gamma) = 67 \pm 7$ keV (one obtains $|g| = 0.22 \pm 0.01$ GeV⁻¹) or⁸ $\Gamma(\omega \rightarrow \pi \gamma) = 890 \pm 90$ keV and SU(3) arguments (in this case $|g| = \frac{1}{3} |g_{\omega\pi\gamma}| = 0.26 \pm 0.02$ GeV⁻¹). Alternatively,¹² one can use simple VMD relations and the experimental values⁸ for $\Gamma(\omega \rightarrow \pi^+ \pi^- \pi^0)$ and $\Gamma(\omega \rightarrow e^+ e^-)$ to obtain $|g| \simeq 0.3$ GeV⁻¹. According to this, we will adopt the value

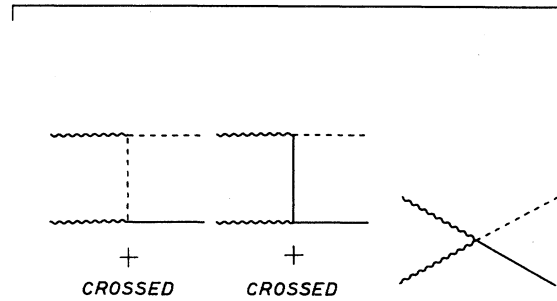


FIG. 2. Gauge-invariant set of diagrams for $\gamma(k) + \gamma(k') \rightarrow \rho^+(p) + \pi^-(q)$.

for $\Gamma(\omega \rightarrow \pi^+ \pi^- \pi^0)$ and $\Gamma(\omega \rightarrow e^+ e^-)$ to obtain $|g| \simeq 0.3 \text{ GeV}^{-1}$. According to this, we will adopt the value

$$g^2 = 0.07 \pm 0.02 \text{ GeV}^{-2} \quad (15)$$

as the most reasonable estimate. Thus, our predictions for the cross sections will be affected by errors $\sim 30\%$, which will be substantially reduced when more accurate data on the $\rho \rightarrow \pi\gamma$ coupling constant become available. On the contrary, the value of the total magnetic moment of the ρ^\pm , $\mu = 1 + \kappa$, is completely unknown. Three main possibilities will be discussed: (i) $\mu = 0$, which corresponds to a pure electric Born model⁴, (ii) $\mu = 1$, as would be the case for charged ρ mesons without anomalous magnetic moment, $\kappa = 0$, and (iii) $\mu = 2$, which corresponds to the most interesting (and probably most realistic) case of ρ^0 -dominated photons (VMD) coupled to charged ρ^\pm mesons through a Yang-Mills coupling.

The numerical results for the differential cross section $d\sigma(\gamma\gamma \rightarrow \rho^\pm \pi^\mp)/d\Omega = 2d\sigma(\gamma\gamma \rightarrow \rho^+ \pi^-)/d\Omega$ have been plotted in Figs. 3(a), 3(b), and 3(c) for total $\gamma\gamma$ center-of-mass energies $W_{\gamma\gamma} = 1.0, 1.3,$ and 1.6 GeV , respectively. The predicted angular distributions have a peculiar shape with a marked forward dip, which, in principle, could be used to test the validity of our model and the presence of additional contributions coming from competing mechanisms. As previously discussed, these are expected to be the formation of $J^{PC}(I^G) = 0^{-+}(1^-)$ and $2^{++}(1^-)$ resonant states. The first possibility leads to isotropic angular distribution, while the second one leads to $\sin^2\theta \cos^2\theta$ (for an A_2 helicity $\lambda = 0$) and to $1 - \cos^4\theta$ (for $\lambda = \pm 2$). The first two cases are clearly distinguishable from our results, Fig. 3, but the latter (possibly more relevant²) is not and requires further discussion.

To this end, we have evaluated the predictions of our model for the angular distribution of the ρ^\pm decay angle θ^* (in the ρ^\pm rest frame). The results for $\mu = 0, 1,$ and 2 are quite similar and have been plotted in Fig. 4 for $W_{\gamma\gamma} = 1.3 \text{ GeV}$. The θ^* angular distributions corresponding to the formation of $J^{PC} = 0^{-+}$ or 2^{++} intermediate states are found to be proportional to $\cos^2\theta^*$ (all ρ mesons are produced in the $\lambda_\rho = 0$ helicity state) or to $\sin^2\theta^*$ ($\lambda_\rho = 0$ is now forbidden), respectively, and have been plotted in Fig. 4 for comparison. The marked difference (similarity) between the $J^{PC} = 2^{++}$ (0^{-+}) contribution and our model is a consequence of the dominant production of zero-helicity ρ mesons in the latter which represents $\sim 80\%$ of the cross sec-

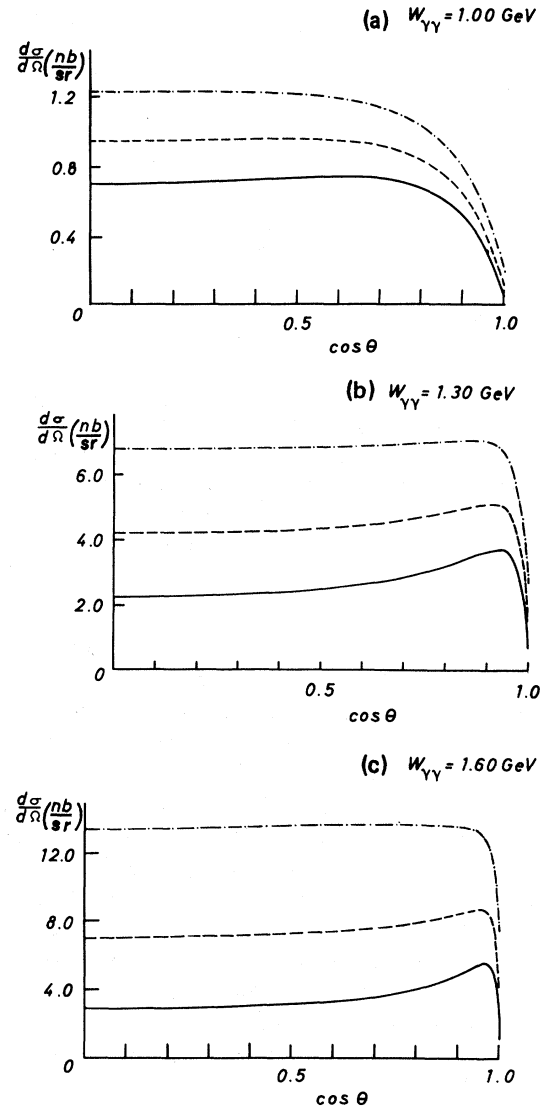


FIG. 3. Differential cross sections $d\sigma(\gamma\gamma \rightarrow \rho^\pm \pi^\mp)/d\Omega$ (in nb/sr) for (a) $W_{\gamma\gamma} = 1 \text{ GeV}$, (b) $W_{\gamma\gamma} = 1.3 \text{ GeV}$, and (c) $W_{\gamma\gamma} = 1.6 \text{ GeV}$. The solid, dashed, and dot-dashed curves are for ρ^\pm magnetic moment $\mu = 0, 1,$ and 2 , respectively.

tions in the whole energy range, $W_{\gamma\gamma} \simeq 1.0$ to 1.6 GeV , and for $\mu = 0, 1,$ or 2 . This makes it possible to distinguish between our mechanism and the potentially dangerous contributions of 2^{++} resonances, such as the A_2 . On the other hand, it also shows that one can neglect any interference between these two contributions due both to the helicity differences and to the predominantly imaginary phase of the A_2 amplitude.

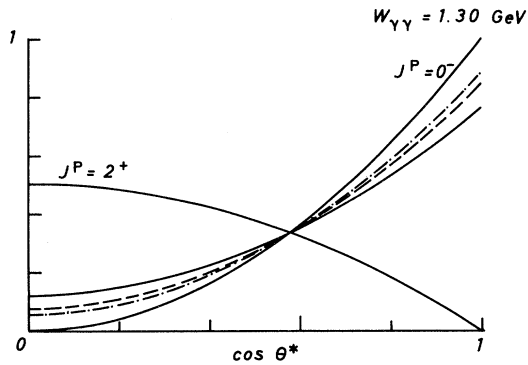


FIG. 4. Angular distribution of the ρ^\pm -decay angle (in the ρ^\pm rest frame) for $W_{\gamma\gamma} = 1.3 \text{ GeV}$. The solid, dashed, and point-dashed curves are for $\mu = 0, 1,$ and $2,$ respectively. The angular distributions expected from resonant decays are labeled with the corresponding quantum numbers $J^P = 0^-$ or 2^+ . Ordinate is in arbitrary units.

The integrated cross section $\sigma(\gamma\gamma \rightarrow \rho^\pm \pi^\mp)$ has been plotted in Fig. 5 for different values of $W_{\gamma\gamma}$ and $\mu = 0, 1, 2$. As expected, it turns out to be rather large (of the same order of that recently measured³ for $\gamma\gamma \rightarrow \pi^+ \pi^- \pi^+ \pi^-$) thus allowing for a reasonably simple experimental detection and accumulation of statistics. Notice however that the reliability of our predictions for the total cross section $\sigma(\gamma\gamma \rightarrow \rho^\pm \pi^\mp)$ decreases when increasing the values of $W_{\gamma\gamma}$. This can be due to the appearance of resonant peaks (which also change the angular distributions) and also to absorption processes⁴ whose strength—rather difficult to estimate—will certainly reduce the values of $\sigma(\gamma\gamma \rightarrow \rho^\pm \pi^\mp)$ for $W_{\gamma\gamma}$ well above threshold.

IV. CONCLUSIONS

A simple Born model based on gauge invariance has been presented in order to describe the main features of the $\gamma\gamma \rightarrow \rho^\pm \pi^\mp$ cross sections not far from threshold. In this energy region one expects the dominance of these Born terms which, eventually, could be superposed to the very small number of resonances coupled both to $\gamma\gamma$ and $\rho\pi$. The value of the total cross section is predicted to be rather large (as in $\gamma\gamma \rightarrow \pi^+ \pi^- \pi^+ \pi^-$), thus allowing

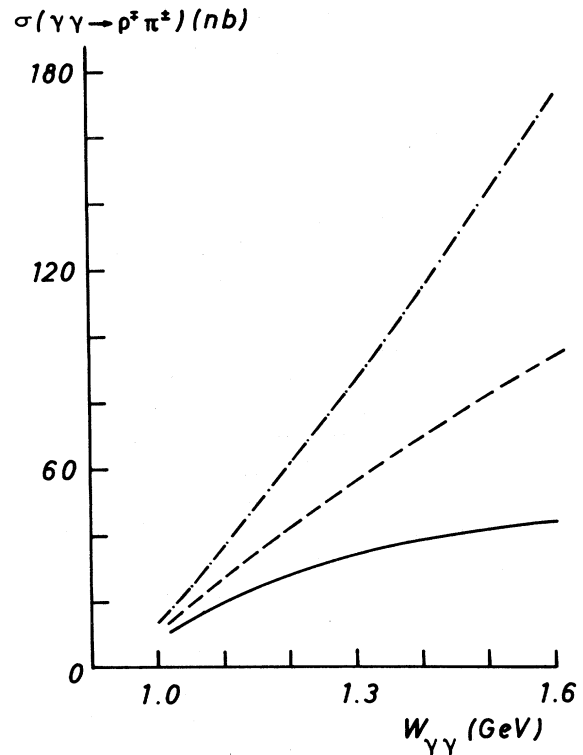


FIG. 5. Total cross section $\sigma(\gamma\gamma \rightarrow \rho^\pm \pi^\mp)$ vs $W_{\gamma\gamma}$ for $\mu = 0$ (solid curve), $\mu = 1$ (dashed curve), and $\mu = 2$ (dot-dashed curve).

for easy experimental detection and good statistics. The angular distribution of the ρ^\pm production angle and the ρ^\pm decay angle (in the ρ^\pm rest frame) are predicted to differ from those of competing mechanisms and can be used to check our model and to establish its range of validity. Finally, the dependence of the differential and total cross sections on the magnetic moment of the charged ρ^\pm ($\mu \equiv 1 + \kappa$, in units of $e/2M$) seems to allow (in particular, when a more accurate value for the $\rho\pi\gamma$ coupling constant g becomes available) for a first determination of this important ρ^\pm -meson property.

ACKNOWLEDGMENT

This work was supported in part by the Instituto de Estudios Nucleares.

- ¹J. H. Field, rapporteur talk at the International Colloquium on Photon-Photon Interactions, Paris, 1981, Report No. DESY 81/037 (unpublished).
- ²D. L. Burke, rapporteur talk at the International Colloquium on Photon-Photon Interactions, Paris, 1981, Report No. SLAC-PUB-2745, 1981 (unpublished); Ch. Berger, Report No. CERN-EP/81-154, 1981 (unpublished).
- ³R. Brandelik *et al.*, Phys. Lett. **B97**, 448 (1980); D. L. Burke *et al.*, *ibid.* **B103**, 153 (1981).
- ⁴D. Lüke and P. Söding, *Springer Tracts in Modern Physics*, edited by G. Höhler (Springer, Berlin, 1971), Vol. 59, p. 39.
- ⁵C. Ayala, A. Bramon, and F. Cornet, Phys. Lett. **107B**, 235 (1981).
- ⁶Y. Goldschmidt and H. R. Rubinstein, Nucl. Phys. **B97**, 445 (1975).
- ⁷S. J. Brodsky, rapporteur talk at the International Colloquium on Photon-Photon Interaction, Paris, 1981, SLAC-PUB-2747, 1981 (unpublished).
- ⁸Particle Data Group, Rev. Mod. Phys. **52**, S1 (1980).
- ⁹G. Bellini *et al.*, Report No. CERN-EP/81-97, 1981 (unpublished); M. Bonesini *et al.*, Phys. Lett. **103B**, 75 (1981).
- ¹⁰T. D. Lee and C. N. Yang, Phys. Rev. **128**, 885 (1962).
- ¹¹D. Berg *et al.*, Phys. Rev. Lett. **44**, 706 (1980).
- ¹²A. Bramon and M. Greco, Phys. Lett. **48B**, 137 (1974); Nuovo Cimento **14A**, 323 (1973).